Effect of Implant Diameter on Biomechanical Response of Straight Multi-Unit Abutments in Mandibular All-on-3: A 3D Finite Element Study

Muhammad Iqbal Ramadhani[1], Kriswanto[1], Febri Budi Darsono [1], Rahmat Doni Widodo[1], J. Jamari[2], Athanasius Priharyoto Bayuseno[2]

[1] Mechanical Engineering, Faculty of Engineering, Universitas Negeri Semarang, Semarang, Central Java, Indonesia.
[2] Mechanical Engineering, Faculty of Engineering, Universitas Diponegoro, Semarang, Central Java, Indonesia.
Email: iqblramadhani09@students.unnes.ac.id

ABSTRACT

This study evaluates the biomechanical performance of varying implant fixture diameters in mandibular edentulous rehabilitation using the All-on-3 concept with straight multi-unit abutments. A three-dimensional finite element model of a mandible segment was constructed and subjected to static occlusal loading conditions derived from clinical bite force data. Three Brånemark-type implants with diameters of 3.75 mm, 4.0 mm, and 5.0 mm were analyzed using ANSYS Workbench to assess von Mises stress, equivalent strain, and factor of safety (FOS) in abutment and screw components. The results revealed that increasing the fixture diameter to 5.0 mm reduced von Mises stress by 12.8- 15.0% in abutments and 17-44.3% in screws across anterior and posterior positions. Similarly, strain decreased by up to 11.1% in abutments and 45.0% in screws. The highest FOS (37.48 for abutment, 25.09 for screw) was recorded at the 5.0 mm diameter, confirming enhanced safety margins. However, posterior implants experienced stress transfer from abutment to screw components as diameter increased, particularly due to local stiffness mismatch and cantilever effects. While all configurations remained below Ti-6Al-4V yield strength, the posterior 3.75 mm setup yielded the lowest FOS (1.45), suggesting a higher mechanical risk. These findings emphasize the need for careful diameter selection in posterior All-on-3 designs.

Keyword: Finite element analysis, All-on-3, mandibular edentulous, full-arch prosthesis, implant diameter, biomechanical.

INTRODUCTION

Total edentulism, or the complete loss of permanent teeth, has wide-ranging consequences for oral functions such as chewing and speech, psychosocial aspects, and overall quality of life. According to the WHO Global Oral Health Status Report 2022, more than 3.5 billion people worldwide suffer from oral health problems with a particularly high prevalence among older people (Jain et al., 2024; Muhammad & Srivastava, 2022). In Indonesia, the 2018 Riset Kesehatan Dasar (Riskesdas) reported that approximately 30 percent of individuals aged over 65 years experienced partial or total tooth loss.

Implant-supported prosthetic approaches have become the preferred method for edentulous rehabilitation due to their high stability and more physiological load distribution than conventional dentures. A systematic review by Hirani et al. (2022) reported a mean implant survival rate of 96.2% over an average 3.35-year follow-up period. Similarly in their meta-analysis, Sánchez-Sánchez-Labrador et al. (2021) found a 95.9% implant and 97.0% prosthetic survival rates. This approach has evolved into the All-on-X system, which enables full-arch rehabilitation using a minimal number of implants. Systems such as All-on-4 and All-on-6 have been extensively studied and proven effective(Zhang et al., 2023). However, the All-on-3 approach which utilizes only three implants is gaining attention due to its cost-effectiveness and procedural simplicity (Afrashtehfar et al., 2022).

All-on-3 is an incredible solution for patients with limited bone volume or systemic conditions that limit extensive surgical intervention. Implants are typically placed exclusively one implant in the anterior region and two implants in the posterior region of the mandible (Gopal et al., 2020; Kanewoff et al., 2024). The reduced number of support points makes the system highly dependent on precise biomechanical planning. The occlusal forces received by the prosthesis are distributed across the three implants creating considerable torsional moments and flexural forces particularly in the posterior region associated with the cantilever effect (Desai et al., 2023).

One of the interesting opportunities offered by the All-on-3 system is its ability to overcome stress concentration at the abutment and screw connections. Lateral and vertical loads can cause screws to loosen or even fracture (Tak et al., 2023; Tribst et al., 2022). Finite Element Analysis (FEA) simulations have reported that peak stress often occurs at the implant neck and screw head, especially under oblique loading conditions as found (Tribst et al., 2021). Therefore, implant geometry specifically the fixture diameter is a crucial factor to be examined.

Implant diameter affects the contact surface area between the implant and the surrounding bone and influences how the mechanical load is distributed(Lee et al., 2021). Qiu et al., (2024) showed that larger diameters can reduce peak stress, enhance load distribution, and improve biomechanical predictability. However, anatomical constraints such as a narrow mandible limit the universal use of large-diameter implants.

In addition to shape and size, the biomechanical performance of implants is highly dependent on material characteristics (Kriswanto et al., 2025). The titanium alloy Ti-6Al-4V is commonly used due to its high strength, corrosion resistance, and long-term biocompatibility (Bocchetta et al., 2021). This alloy's structural and microstructural stability in complex physiological environments (Biomedical Applications et al., 2023). For the prosthetic framework, cobalt-chromium alloy is preferred for its high stiffness and ability to resist elastic deformation under long cantilever extensions (Fratila et al., 2023; Garcia-Falcon et al., 2021).

FEA is a widely used non-invasive method for evaluating stress distribution in implant systems. It allows detailed simulations of parameters such as von Mises stress and equivalent strain with reasonable control over variables (Alemayehu et al., 2021). An essential aspect of accurate FEA modeling is the mechanical property representation of bone. While many previous studies have used isotropic assumptions, cortical bone exhibits orthotropic behavior. Orthotropic properties can significantly improve stress prediction accuracy in peri-implant regions (Paracchini et al., 2020).

This study aims to evaluate the effect of implant diameter variation (3.75 mm, 4.0 mm, and 5.0 mm) on the distribution of von Mises stress equivalent strain and safety factor in the abutment and screw components of the All-on-3 mandibular edentulous system. A three-dimensional model reconstructed from CBCT scans was developed where bone was modeled as orthotropic and implant components were made of Ti-6Al-4V with a CoCr framework. Simulations were conducted using ANSYS Workbench 2024 under three-directional static loading conditions based on in vivo occlusal data.

The findings of this study are expected to provide deeper insights into the optimal implant design for All-on-3 applications and contribute to reducing the risk of long-term mechanical failure, particularly in abutment and screw components.

METHODS

A three-dimensional finite element model of the edentulous mandibular segment was developed based on CBCT reconstruction. The mandible consisted of a 2 mm cortical layer and a 15 mm cancellous layer (Tribst et al., 2022). This model represented the mandibular second premolar region and was used to place three Brånemark System Mk III implants with three diameter variations, namely 3.75 mm, 4.0 mm, and 5.0 mm. The fixture length was set constant at 10 mm with a V-thread design, a pitch of 0.6 mm, and a thread depth of 0.3 mm. The design referred to the commercial approach of Nobel Biocare (2024) with straight multi-unit abutments made of Ti-6Al-4V modified for each diameter. Abutments for the 3.75 mm and 4.0 mm diameters used the same platform size, while the 5.0 mm diameter used a larger abutment to match the implant dimensions

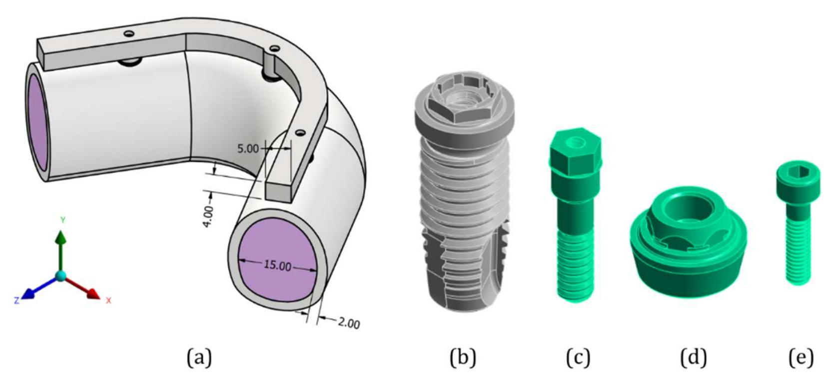

Figure 1. Components of the Dental Implant FE Model: (a) Full bone-implant assembly; (b) Fixture; (c) Screw between abutment and fixture; (d) Abutment; (e) Screw between framework and abutment

The implant component design in this study refers to the commercial design approach of Nobel Biocare (2024) with fixtures resembling Brånemark System Mk III TiUnite and adapted straight multi-unit abutments. The fixture is bone-level with an external hexagon connection to the abutment. Implants were placed in an All-on-3 configuration with three diameter variations, namely 3.75 mm, 4.0 mm, and 5.0 mm. The fixture length was consistently 10 mm with a V-shaped thread form, pitch 0.6 mm, and thread depth 0.3 mm. Abutments for 3.75 mm and 4.0 mm diameters used the exact dimensions, while for the 5.0 mm diameter, an abutment with a broader platform was used to match the implant dimensions.

All components were modeled using Autodesk Inventor Professional 2025 software and exported to ANSYS Workbench 2024 for static linear FEA simulation. The implant and prosthesis components were modeled as isotropic linear elastic materials. In contrast, cortical and trabecular bones were modeled as orthotropic homogeneous elastic materials based on data from Ding et al, (2014). The mechanical properties of all materials are shown in Table 1.

The characteristics of the material used for the implant complex are Ti-6Al-4V material. The properties of the material model used in this study are orthotropic, homogeneous, and linearly elastic for the bone model. The implant complex is isotropic, homogeneous, and linearly elastic as presented in Table 1.

This study used a linear elastic-based finite element analysis (FEA) approach for numerical analysis. The structural geometry was modeled in the form of small elements, which were then connected into a global system through the formation of the element stiffness matrix as expressed by the following equation (Jawad et al, 2017):

$$[K_e][q]=[F] \tag{1}$$

Table 1. Material Properties

Component of Model	Young's Modulus, E (GPa)	Shear Modulus, G (GPa)	Poisson's Ratio, ν	Density (g/cc)	References
Cortical	$E_x = 12.7$	$G_{xy} = 5.5$	$\nu_{xy} = 0.31$	-	
	$E_y = 22.8$	$G_{yz} = 7.4$	$\nu_{yz} = 0.28$	-	(Ding et al., 2014)
	$E_z = 17.9$	$G_{xz} = 5.0$	$\nu_{xz} = 0.18$	-	
Cancellous	$E_x = 0.511$	$G_{xy} = 0.434$	$\nu_{xy} = 0.31$	-	
	$E_y = 0.907$	$G_{yz} = 0.081$	$\nu_{yz} = 0.30$	-	(Ding et al., 2014)
	$E_z = 0.114$	$G_{xz} = 0.078$	$\nu_{xz} = 0.22$	-	
Ti-6Al-4V	113.8	-	0.342	4.43	(ASM Aerospace Specification Metals Inc., n.d.)
Co-Cr	210	-	0.29	10	(Lanza et al., 2023)

Where *[Ke]* is the element stiffness matrix, *[q]* is the nodal displacement vector and *[F]* is the force vector acting on those points. The matrix *[Ke]* is calculated through volumetric integration:

$$[K_e] = \int_V [B]^T [D][B]\, dV \tag{2}$$

According to Hooke's Law. *[B]* represents the strain-displacement matrix and *[D]* is the constitutive material matrix representing the relationship between stress and strain.

Furthermore, in this FEA analysis one of the main variables observed was von Mises stress. This stress was calculated based on the stress components in the X, Y, and Z axes (σ_x, σ_y, σ_z), as well as the shear stress components (τ_{xy}, τ_{yz}, τ_{zx}) on their respective planes. The formula used refers to (Budynas & Nisbett, 2015):

$$\sigma' = \frac{1}{\sqrt{2}}\left[\left(\sigma_x - \sigma_y\right)^2 + \left(\sigma_y - \sigma_z\right)^2 + (\sigma_z - \sigma_x)^2 + 6\left(\tau_{xy}^2 + \tau_{yz}^2 + \tau_{zx}^2\right)\right]^{1/2} \tag{3}$$

Where σ_x, σ_y, dan σ_z are standard stress components in the X, Y, and Z axes respectively while τ_{xy}, τ_{yz}, dan τ_{zx} are the shear stress components occurring on the xy, yz, and zx planes. The equivalent von Mises stress (σ') represents the overall combined stress condition in the structure.

In addition to stress, the other variable analyzed was the von Mises equivalent strain. The calculation of this strain refers to the formula (ANSYS Inc., 2024):

$$\varepsilon_{eq} = \frac{1}{\sqrt{2}(1+\nu)}\left[\left(\varepsilon_x - \varepsilon_y\right)^2 + \left(\varepsilon_y - \varepsilon_z\right)^2 + (\varepsilon_z - \varepsilon_x)^2 + \frac{3}{2}\left(\gamma_{xy}^2 + \gamma_{yz}^2 + \gamma_{xz}^2\right)\right]^{1/2} \tag{4}$$

Considering the standard strain components (ε_x, ε_y, ε_z) and shear strains (γ_{xy}, γ_{yz}, γ_{xz}). This calculation provides the ε_{eq} value as the total equivalent strain representing cumulative deformation with ν as the effective Poisson's ratio of the material.

Mesh quality evaluation used skewness metrics as the assessment standard. Based on ANSYS processing results, the average skewness values for the three diameter variations ranged from 0.65208 to 0.67065, with a minimum value for the 3.75 mm diameter of 0.015456. This range is considered reasonable based on the mesh quality classification by ANSYS (2024). The final nodes for the 3.75 mm, 4.0 mm, and 5.0 mm diameters were 550429, 604613, and 584572, respectively. Meanwhile, the elements were 341154, 377860, and 360992, respectively. Figure 2 illustrates the mesh distribution applied in the model.

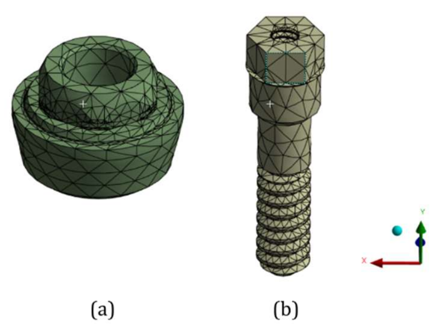

Figure 2. Meshing of the Abutment and Abutment screw

The inferior surface of the bone model was fixed in all degrees of freedom. Vertical loading was applied to three different areas: anterior (incisor), right posterior (right molar), and left posterior (left molar). Based on clinical data from healthy males aged 20–40 years, the average bite force was 204.1 N (incisor), 544.1 N (left molar), and 546.2 N (right molar). These values were converted from kilogram-force (kp) to Newton (N) using one kp ≈ 9.81 N. The loading vectors were directed according to the buccal–distal–occlusal orientation as in functional occlusion characteristics as illustrated in Figure 3.

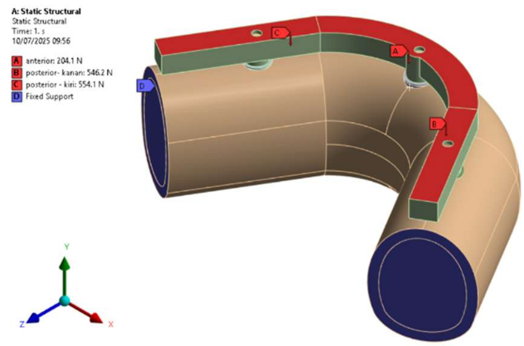

Figure 3. Boundary Conditions and Loading of the Dental Implant Model

All interfaces between components, including abutment and fixture connection screw and abutment, as well as bar and abutment, were modeled as perfectly bonded (Lee et al., 2021). One hundred percent osseointegration between the fixture and bone was assumed based on the approach by Chen et al., (2025). This static simulation did not include micromotion fatigue and nonlinear material behavior (Figure 3).

This study analyzed biomechanical responses in the form of von Mises stress and von Mises strain occurring at the connection between the abutment and abutment screw due to variations in the implant fixture diameter. The evaluation was conducted using the Finite Element Analysis (FEA) method. In addition, the maximum von Mises stress values obtained were further analyzed using the Safety Factor (FOS) approach by comparing them to the yield strength of Ti-6Al-4V material at 880 MPa (ASM Aerospace Specification Metals Inc. n.d.). The calculation formula refers to (Budynas & Nisbett, 2015):

$$n_d = \frac{S}{\sigma} \quad (5)$$

Where n_d is *safety factor* FOS, S is yield strength, and σ is the allowable stress, which in this study is the maximum von Mises stress.

Table 2. Mesh convergence analysis based on maximum Von Mises stress values.

Type Mesh	Mesh Sizing (mm)	Number of Element	Number of Nodes	Von Mises Stress Abutment, σ' (MPa)	Von Mises Stress Screw, σ' (MPa)	Percentage Variation of Abutment (%)	Percentage Variation of Screw (%)
Quadratic Tetrahedral	0.95	337530	544734	617.85	302.63	-	-
Quadratic Tetrahedral	0.94	341154	550429	608.29	292.69	-1.55%	-3.28%
Quadratic Tetrahedral	0.93	344172	554517	584.44	288.48	-3.92%	-1.44%

RESULT & DISCUSSION

The results of the finite element analysis (FEA) simulation showed that the variation in implant fixture diameter significantly influenced the distribution of von Mises stress and equivalent strain on the abutment and screw components in the All-on-3 system. For the anterior position, the highest maximum stress value on the abutment was recorded at a diameter of 4.0 mm at 65.896 MPa. In comparison, the lowest stress occurred at a diameter of 3.75 mm at 52.96 MPa. Interestingly, when the diameter was increased to 5.0 mm, there was a significant decrease in screw stress from 34.816 MPa to only 19.396 MPa. Strain on the screw also decreased sharply from 0.0003757 to 0.0002064. This indicates that a larger diameter is more effective in damping loads in the anterior area.

In the proper posterior position, where an occlusal force of 546.2 N was applied, there was a trend of decreasing stress on the abutment as the fixture diameter increased. Stress decreased from 569.4 MPa at a diameter of 3.75 mm to 511.88 MPa at a diameter of 5.0 mm. Abutment strain also decreased from 0.0051115 to 0.0046328. However, the stress on the screw increased from 283.63 MPa (4.0 mm) to 331.77 MPa (5.0 mm). Although the strain on the screw remained at 0.002511, this increase in stress indicates a redistribution of load from the abutment to the screw, possibly due to changes in local stiffness in the joint system.

Meanwhile, in the left posterior position, the stress and strain distribution pattern followed a trend like the right side. Abutment stress decreased from 608.29 MPa (3.75 mm) to 572.77 MPa (5.0 mm), and strain decreased from 0.0054917 to 0.0051693. However, for the screw stress progressively increased from 281.93 MPa to 327.35 MPa, followed by an increase in strain from 0.002575 to 0.002942. This shows that in larger diameters, some of the force that was initially absorbed by the abutment began to shift to the screw due to the influence of geometry and local stiffness, particularly in the posterior load position near the cantilever.

Table 3. FEA Results of Stress and Strain Different Fixture Diameters di Position 1 (Anterior)

Diameter (mm)	Max Von Mises Stress, σ' (MPa)		Max Von Mises Strain, ε_{eq}	
	Abutment 1	Screw 1	Abutment 1	Screw 1
3.75	52.96	26.174	0.00050065	0.0003126
4.0	65.896	34.816	0.00061386	0.0003757
5.0	57.488	19.396	0.00054567	0.0002064

Table 4. FEA Results of Stress and Strain Different Fixture Diameters di Position 2 (Right Posterior)

Diameter (mm)	Max Von Mises Stress, σ' (MPa)		Max Von Mises Strain, ε_{eq}	
	Abutment 2	Screw 2	Abutment 2	Screw 2
3.75	569.4	292.69	0.0051115	0.002593
4.0	533.32	283.63	0.0047962	0.002511
5.0	511.88	331.77	0.0046328	0.002511

Table 5. FEA Results of Stress and Strain Different Fixture Diameters di Position 3 (Left Posterior)

Diameter (mm)	Max Von Mises Stress, σ′ (MPa)		Max Von Mises Strain, ε_{eq}	
	Abutment 3	Screw 3	Abutment 3	Screw 3
3.75	608.29	281.93	0.0054917	0.002575
4.0	576.09	302.12	0.0052276	0.002688
5.0	572.77	327.35	0.0051693	0.002942

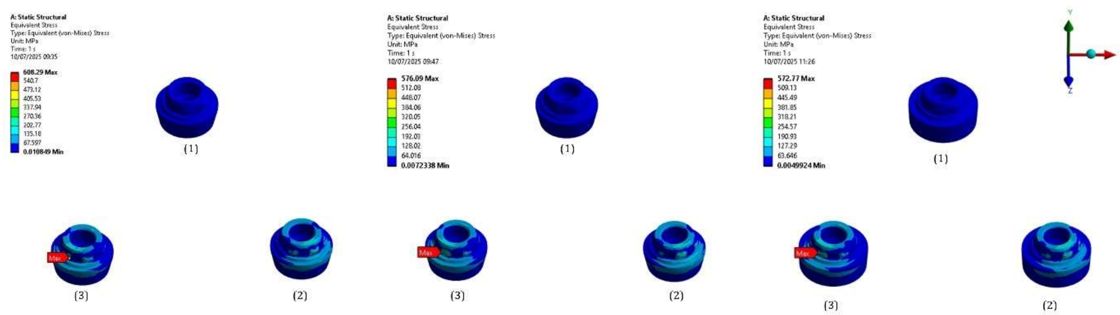

(a) (b) (c)

Figure 4. Von Mises stress on abutment: (a) at 3.75 mm diameter, (b) at 4.0 mm, (c) at 5.0 mm.

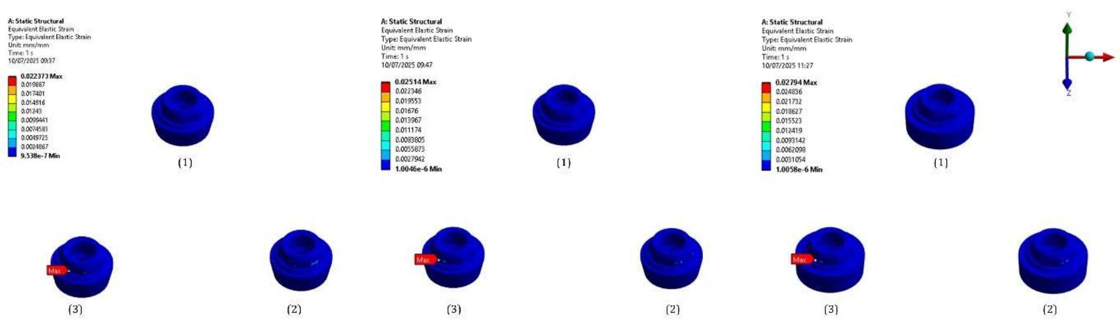

(a) (b) (c)

Figure 5. Von Mises strain on abutment: (a) at 3.75 mm diameter, (b) at 4.0 mm, (c) at 5.0 mm.

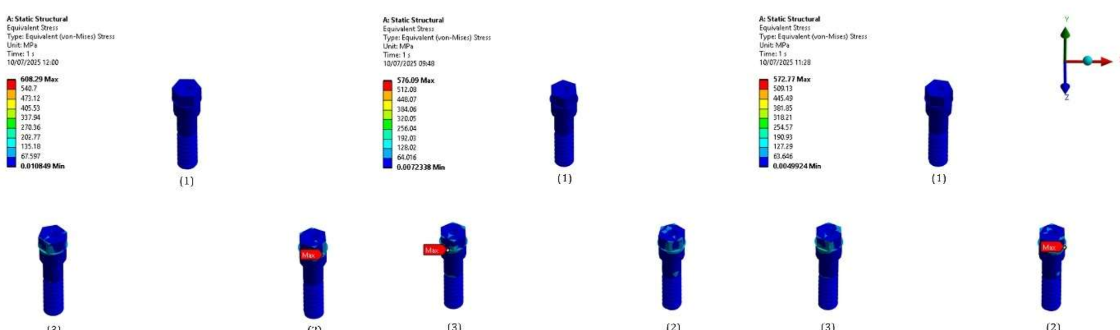

(a) (b) (c)

Figure 6. Von Mises stress on abutment screw: (a) at 3.75 mm diameter, (b) at 4.0 mm, (c) at 5.0 mm.

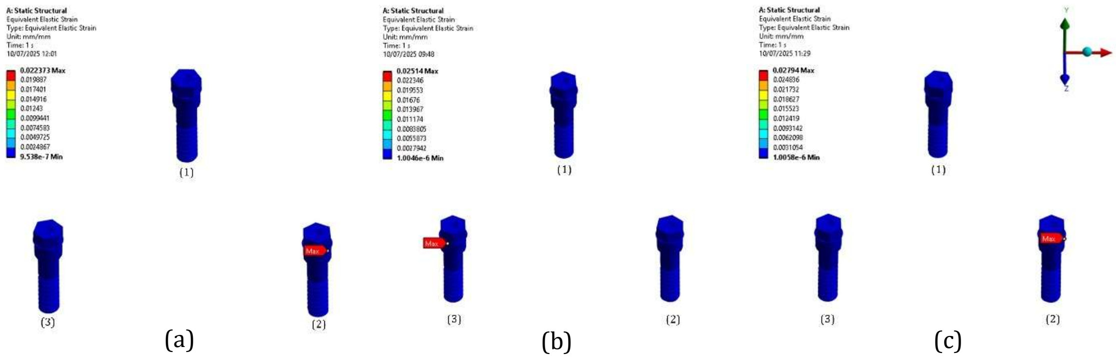

Figure 6. Von Mises strain on abutment screw: (a) at 3.75 mm diameter, (b) at 4.0 mm, (c) at 5.0 mm.

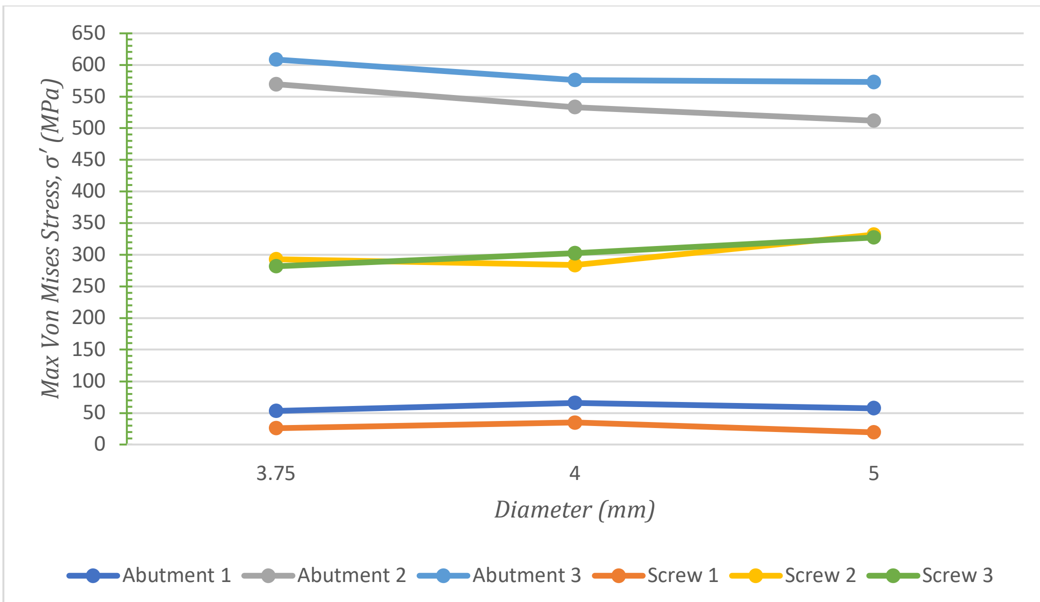

Figure 5. Graph of fixture diameter vs von mises stress

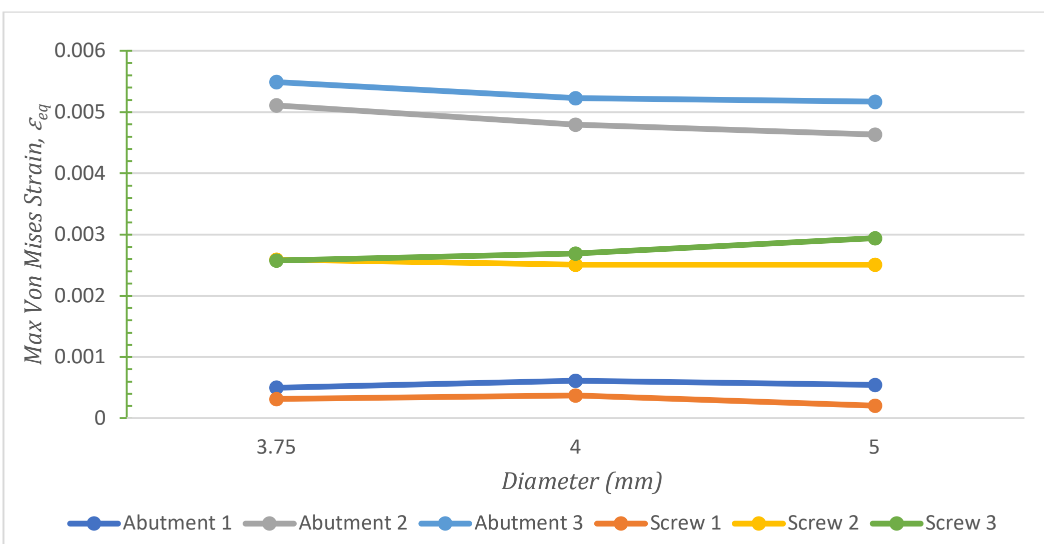

Figure 6. Graph of fixture diameter vs von mises strain

Safety factor evaluation was conducted by comparing the maximum stress to the yield strength of Ti-6Al-4V material at 880 MPa. The safety factor calculation (FOS = 880/σ) was performed for each diameter and position combination. The results showed that all configurations had FOS > 1, meaning they were still within the elastic zone of the material. The anterior position showed the highest safety margin, particularly in the 5.0 mm screw with a FOS of 45.37. On the other hand, the smallest safety margin was found in the abutment in the left posterior position with a diameter of 3.75 mm at 1.45. This indicates that although all configurations are structurally safe, the safety margin in the posterior position needs further attention.

When compared across positions, the posterior area consistently showed higher stress and strain values than the anterior, which corresponds to the higher occlusal forces in that area. One interesting point is that the 4.0 mm diameter, which logically lies in the middle, produced the highest stress values in the anterior position. This suggests that increasing fixture diameter does not always result in a linear biomechanical effect and should be adjusted based on the overall system proportion.

From a biomechanical perspective, increasing the fixture diameter proved to help reduce the load on the abutment. However, an increase in diameter can also cause the screw to receive additional stress, especially in the posterior area. This change is likely caused by using a wider platform abutment in the 5.0 mm diameter, which alters the load distribution and increases local stiffness. Although all stress values are below the Ti-6Al-4V yield limit, the abutment stress approaching 69 percent yield strength in the 3.75 mm configuration in the left posterior position shows a relatively low safety margin.

Graphical visualization of the stress trends shows a pattern consistent with the numerical findings. The increasing fixture diameter in the abutment tends to reduce maximum stress, especially on the posterior side. However, in the screw, the opposite pattern occurs; stress increases with increasing diameter, particularly in the right and left posterior. This confirms that although a large diameter is beneficial for the abutment, special attention must be given to the design of the screw and its interface to avoid potential new risks.

The results of this simulation provide a clear picture of the effect of fixture diameter on the load received by the All-on-3 implant system. One of the most noticeable findings is that the larger the diameter, the more the load received by the abutment tends to decrease, especially in the posterior area, which receives the highest chewing force. This is logical because a larger fixture has a wider contact surface to distribute the load more evenly.

Even so, the effect of increasing diameter is not entirely positive. An increase in fixture diameter causes stress on the screw to increase, especially in the posterior. This may be because the stiffer structure shifts part of the load to the screw, which is more flexible. In other words, changing one part of the system can shift the load to another part that may not be designed to withstand the additional pressure.

In addition, the 4.0 mm diameter, which in theory is intermediate, does not always produce the best performance. For example, this configuration recorded the highest stress and strain in the anterior position. This shows that moderate size does not always mean the optimal compromise solution. Overall design adjustment seems more important than simply enlarging or reducing the fixture diameter.

From a safety standpoint, all configurations tested were still within the elastic limit of Ti-6Al-4V. This means mechanically, all can be considered safe to use. However, when considering the safety margin, the 3.75 mm diameter in the posterior position needs further attention because the stress value approaches the threshold. This condition may not be critical for patients with good bone and normal loads, but may be risky in cases with poor bone quality or excessive chewing loads.

Although this study provides valuable biomechanical insights into the effect of implant diameter in the All-on-3 mandibular system, several limitations and research opportunities remain. Simulations were performed under static loading conditions, which do not fully reflect the dynamic and cyclic nature of masticatory forces encountered in clinical scenarios; therefore, fatigue-related performance over time could not be evaluated.

Furthermore, the model assumed idealized conditions, including complete osseointegration and absence of soft tissue, anatomical variability, or full prosthetic superstructures, which may limit the clinical translatability of the findings. There is a significant research gap in understanding how variations in screw design or screw-support interface can affect load redistribution, especially in systems using large-diameter implants where local stiffness can shift pressure toward the screw. Future research should incorporate cyclic loading protocols, fatigue simulations, and a wider variety of designs to improve the clinical relevance and long-term predictive accuracy of All-on-3 biomechanical models.

Furthermore, the influence of bone quality factors (cortical vs. spongy), bone resorption status, and multipoint loading direction has not been fully explored. Adding these variables can provide a more comprehensive biomechanical picture of the All-on-3 system. Finally, modeling the complete prosthesis, including the denture bar and soft tissue elements, can contribute significantly to the clinical validity of this simulation.

CONCLUSION

Based on the FEA findings, this study presents the following conclusions:

1. An increase in fixture diameter up to 5.0 mm was proven to reduce stress and strain on the abutment in all positions. In the anterior region stress decreased by 12.8 percent and strain by 11.1 percent. In the right posterior stress on the abutment was reduced by 10.1 percent and in the left posterior by 5.8 percent. This indicates that larger diameters are more effective in reducing abutment loads, especially in the anterior area.
2. Conversely the effect on the screw was different. In the anterior region stress and strain decreased significantly by 44.3 percent and 45.0 percent, respectively. However, in the right posterior stress increased by 17.0 percent and in the left posterior stress increased by 16.1 percent with strain increasing by 14.3 percent. This indicates a shift in load to the screw due to increased abutment stiffness which must be anticipated in joint system design.
3. The 5.0 mm diameter yielded the highest safety factor values namely 37.48 on the abutment and 25.09 on the screw compared to the 3.75 mm diameter (28.59 on the abutment and 16.60 on the screw) and 4.0 mm diameter (28.60 on the abutment and 16.67 on the screw) showing an improvement in mechanical stability.
4. Von Mises strain decreased with increasing fixture diameter by 23.7 percent on the abutment and 33.1 percent on the screw with a distribution pattern that followed the stress trend. Overall, the 5.0 mm diameter showed the best biomechanical performance in all positions particularly in reducing the load on the abutment. However the increase in diameter was also accompanied by the risk of increased load on the screw so the screw–abutment connection design needs further attention in the All-on-3 system.

REFERENCE

Afrashtehfar, K. I., Moawad, R. A., Eddin, A. W. F., & Wang, H. L. (2022). Mandibular full-arch fixed prostheses supported by three-dental-implants: A protocol of an overview of reviews. *PLOS ONE*, *17*(4), e0265491. https://doi.org/10.1371/JOURNAL.PONE.0265491

Alemayehu, D.-B., Jeng, Y.-R., Alemayehu, D.-B. ;, & Jeng, Y.-R. (2021). Three-Dimensional Finite Element Investigation into Effects of Implant Thread Design and Loading Rate on Stress Distribution in Dental Implants and Anisotropic Bone. *Materials 2021, Vol. 14, Page 6974*, *14*(22), 6974. https://doi.org/10.3390/MA14226974

ANSYS Inc. (2024). *Chapter 17: Postprocessing in ANSYS Mechanical APDL 2024 R2 Theory References*. https://ansyshelp.ansys.com/public/account/secured?returnurl=////////Views/Secured/corp/v242/en/ans_thry/thy_post12.html

ASM Aerospace Specification Metals Inc. (n.d.). *Titanium Ti-6Al-4V (Grade 5), Annealed*. https://asm.matweb.com/search/SpecificMaterial.asp?bassnum=mtp641

Biomedical Applications, A., Antoniac, V., Marin, E., & Lanzutti, A. (2023). Biomedical Applications of Titanium Alloys: A Comprehensive Review. *Materials 2024, Vol. 17, Page 114*, *17*(1), 114. https://doi.org/10.3390/MA17010114

Bocchetta, P., Chen, L. Y., Tardelli, J. D. C., Dos Reis, A. C., Almeraya-Calderón, F., & Leo, P. (2021). Passive Layers and Corrosion Resistance of Biomedical Ti-6Al-4V and β-Ti Alloys. *Coatings 2021, Vol. 11, Page 487*, *11*(5), 487. https://doi.org/10.3390/COATINGS11050487

Budynas, R. G., & Nisbett, J. K. (2015). *Shigley's Mechanical Engineering Design, Tenth Edition*. McGraw-Hill Education.

Chen, X., Xu, Z., Gai, K., Pei, X., Li, R., & Wan, Q. (2025). Biomechanical analysis of All-on-4 implant supported framework using different materials across various clinical practice. *BMC Oral Health*, *25*(1), 1–10.

https://doi.org/10.1186/S12903-025-05928-0/FIGURES/8

Desai, S. R., Koulgikar, K. D., Alqhtani, N. R., Alqahtani, A. R., Alqahtani, A. S., Alenazi, A., Heboyan, A., Fernandes, G. V. O., & Mustafa, M. (2023). Three-Dimensional FEA Analysis of the Stress Distribution on Titanium and Graphene Frameworks Supported by 3 or 6-Implant Models. *Biomimetics*, *8*(1), 1–25. https://doi.org/10.3390/biomimetics8010015

Ding, X., Liao, S.-H., Zhu, X.-H., & Wang, H.-M. (2014). Influence of Orthotropy on Biomechanics of Peri-Implant Bone in Complete Mandible Model with Full Dentition. *BioMed Research International*, *2014*(1), 709398. https://doi.org/10.1155/2014/709398

Fratila, A., Jimenez-Marcos, C., Mirza-Rosca, J. C., & Saceleanu, A. (2023). Mechanical properties and biocompatibility of various cobalt chromium dental alloys. *Materials Chemistry and Physics*, *304*, 127867. https://doi.org/10.1016/J.MATCHEMPHYS.2023.127867

Garcia-Falcon, C. M., Gil-Lopez, T., Verdu-Vazquez, A., & Mirza-Rosca, J. C. (2021). Electrochemical characterization of some cobalt base alloys in Ringer solution. *Materials Chemistry and Physics*, *260*, 124164. https://doi.org/10.1016/J.MATCHEMPHYS.2020.124164

Gopal, T. M., Rohinikumar, S., Thiyaneswaran, N., & Maiti, S. (2020). Effect of submandibular fossa on implant length in the posterior mandibular region. *Journal of Long-Term Effects of Medical Implants*, *30*(3), 219–226. https://doi.org/10.1615/JLONGTERMEFFMEDIMPLANTS.2020035970,

Hirani, M., Devine, M., Obisesan, O., & Bryant, C. (2022). The use of three implants to support a fixed prosthesis in the management of the edentulous mandible: a systematic review. *International Journal of Implant Dentistry 2022 8:1*, *8*(1), 1–11. https://doi.org/10.1186/S40729-022-00423-5

Jain, N., Dutt, U., Radenkov, I., & Jain, S. (2024). WHO's global oral health status report 2022: Actions, discussion and implementation. *Oral Diseases*, *30*(2), 73–79. https://doi.org/10.1111/odi.14516

Kanewoff, E., Alhallak, R., de Carvalho Machado, V., & Chrcanovic, B. R. (2024). Immediate implant placement in the anterior mandible: a cone beam computed tomography study. *BMC Oral Health*, *24*(1), 1–12. https://doi.org/10.1186/S12903-024-04111-1/TABLES/7

Kriswanto, Jamari, Bayuseno, A. P., Setiawan, F., Fitriyana, D. F., Huda, K., Widodo, R. D., Dhiaulhaque, & Al Afkar, N. B. (2025). Stress and Displacement Simulation of the Posterior Dental Implants on Variations of Applied Materials and Temperatures. *Journal of Advanced Research in Applied Mechanics*, *135*(1), 164–179. https://doi.org/10.37934/ARAM.135.1.164179

Lanza, A., De Stefano, M., & Ruggiero, A. (2023). Investigating the optimal design of all-on-four technique adopting finite element analysis: the aspect of framework material, kind and position of implants. *Biomedical Engineering Advances*, *6*(June), 100110. https://doi.org/10.1016/j.bea.2023.100110

Lee, H., Jo, M., & Noh, G. (2021). Biomechanical effects of dental implant diameter, connection type, and bone density on microgap formation and fatigue failure: A finite element analysis. *Computer Methods and Programs in Biomedicine*, *200*, 105863. https://doi.org/10.1016/J.CMPB.2020.105863

Paracchini, L., Barbieri, C., Redaelli, M., Di Croce, D., Vincenzi, C., & Guarnieri, R. (2020). Finite Element Analysis of a New Dental Implant Design Optimized for the Desirable Stress Distribution in the Surrounding Bone Region. *Prosthesis 2020, Vol. 2, Pages 225-236*, *2*(3), 225–236. https://doi.org/10.3390/PROSTHESIS2030019

Qiu, P., Cao, R., Li, Z., & Fan, Z. (2024). A comprehensive biomechanical evaluation of length and diameter of dental implants using finite element analyses: A systematic review. *Heliyon*, *10*(5). https://doi.org/10.1016/j.heliyon.2024.e26876

Sánchez-Labrador, L., Molinero-Mourelle, P., Brinkmann, J. C. B., Prados-Frutos, J. C., Gómez-Polo, M., & Martínez-González, J. M. (2021). Clinical Behavior and Complications of Mandibular Full-Arch Fixed Dental Prostheses Supported by Three Dental Implants. A Systematic Review and Meta-Analysis. *Biology 2021, Vol. 10, Page 308*, *10*(4), 308. https://doi.org/10.3390/BIOLOGY10040308

Tak, S., Jeong, Y., Kim, J. E., Kim, J. H., & Lee, H. (2023). A comprehensive study on the mechanical effects of implant-supported prostheses under multi-directional loading and different occlusal contact points. *BMC Oral Health*, *23*(1), 1–10. https://doi.org/10.1186/S12903-023-03016-9/FIGURES/12

Tribst, J. P. M., Dal Piva, A. M. de O., da Silva-Concílio, L. R., Ausiello, P., & Kalman, L. (2021). Influence of Implant-Abutment Contact Surfaces and Prosthetic Screw Tightening on the Stress Concentration, Fatigue Life and Microgap Formation: A Finite Element Analysis. *Oral*, *1*(2), 88–101. https://doi.org/10.3390/oral1020009

Tribst, J. P. M., de Morais, D. C., de Matos, J. D. M., Lopes, G. da R. S., Dal Piva, A. M. de O., Borges, A. L. S., Bottino, M. A., Lanzotti, A., Martorelli, M., & Ausiello, P. (2022a). Influence of Framework Material and Posterior Implant Angulation in Full-Arch All-on-4 Implant-Supported Prosthesis Stress Concentration. *Dentistry Journal 2022, Vol. 10, Page 12*, *10*(1), 12. https://doi.org/10.3390/DJ10010012

Tribst, J. P. M., de Morais, D. C., de Matos, J. D. M., Lopes, G. da R. S., Dal Piva, A. M. de O., Borges, A. L. S., Bottino, M. A., Lanzotti, A., Martorelli, M., & Ausiello, P. (2022b). Influence of Framework Material and Posterior Implant Angulation in Full-Arch All-on-4 Implant-Supported Prosthesis Stress Concentration. *Dentistry Journal*, *10*(1). https://doi.org/10.3390/dj10010012

Zhang, Y., Li, S., Di, P., Zhang, Y., Wu, A., & Lin, Y. (2023). Comparison of 4- or 6-implant supported immediate full-arch fixed prostheses: A retrospective cohort study of 217 patients followed up for 3–13 years. *Clinical Implant Dentistry and Related Research*, *25*(2), 381–397. https://doi.org/10.1111/CID.13170,